ACS Chemical Neuroscience

Research Article

Cite This: ACS Chem. Neurosci. 2019, 10, 2022−2032

pubs.acs.org/chemneuro

Characterization of a Multiple-Scan-Rate Voltammetric Waveform for Real-Time Detection of Met-Enkephalin

S. E. Calhoun, C. J. Meunier, C. A. Lee, G. S. McCarty, and L. A. Sombers*

Department of Chemistry, North Carolina State University, Raleigh, North Carolina 27695, United States

ABSTRACT: Opioid peptides are critically involved in a variety of physiological functions necessary for adaptation and survival, and as such, understanding the precise actions of endogenous opioid peptides will aid in identification of potential therapeutic strategies to treat a variety of disorders. However, few analytical tools are currently available that offer both the sensitivity and spatial resolution required to monitor peptidergic concentration fluctuations *in situ* on a time scale commensurate with that of neuronal communication. Our group has developed a multiple-scan-rate waveform to enable real-time voltammetric detection of tyrosine containing neuropeptides. Herein, we have evaluated the waveform parameters to increase sensitivity to methionine-enkephalin (M-ENK), an endogenous opioid neuropeptide implicated in pain, stress, and reward circuits. M-ENK dynamics were monitored in adrenal gland tissue, as well as in the dorsal striatum of anesthetized and freely behaving animals. The data reveal cofluctuations of catecholamine and M-ENK in both locations and provide measurements of M-ENK dynamics in the brain with subsecond temporal resolution. Importantly, this work also demonstrates how voltammetric waveforms can be customized to enhance detection of specific target analytes, broadly speaking.

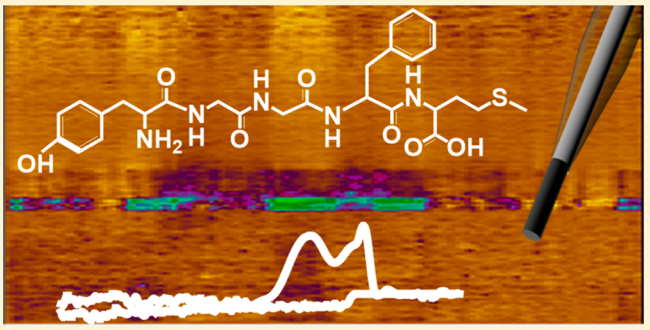

KEYWORDS: *carbon fiber, opioid, chromaffin cell, dopamine, cyclic voltammetry, microelectrode, FSCV*

INTRODUCTION

Endogenous opioid peptides modulate a wide range of physiological functions including pain and reward processing, emotion, feeding behavior, and gastrointestinal activity by acting on the mu, delta, and kappa receptors (MOR, DOR, and KOR, respectively).[1−5] These receptors are differentially expressed throughout the brain and peripheral nervous system.[6−8] Mesolimbic opioid peptides are important mediators of hedonic and motivational aspects of reward processing,[1−5] and aberrant opioid activity in the mesolimbic region is heavily implicated in drug addiction and drug-mediated reinforcing behaviors.[9−14] However, the precise action of these opioid peptides and their interaction with mesolimbic dopamine (DA) remains ambiguous, despite nearly four decades of research. This is largely due to the paucity of techniques for direct detection of opioid peptides *in situ*.

The complexity of the endogenous opioid system presents many hurdles when using existing approaches to dissect the action of specific opioid peptides at specific receptors (or receptor subtypes). Unlike receptors for many other small molecular transmitters, no endogenous opioid peptide family is associated exclusively with any one receptor type.[15] Thus, even the complete and instantaneous blockade of a specific receptor type does not necessarily eliminate the action of a given opioid peptide. Similarly, quantification of mRNA expression and immunohistochemistry are often used to identify neurons that presumably contain the known opioid precursors: pre-proENK, pre-proopiomelanocortin, and pre-prodynorphin. However, cleavage of these larger molecules yields a variety of peptides that elicit a range of physiological responses.[16] In fact, individual fragments from a given prohormone can generate opposing actions at postsynaptic cells in the brain.[15,17] As such, identification of neurons that synthesize precursor molecules provides no information on the contribution of specific opioid peptides to brain function or whether release occurs in the somatodendritic region or at projection targets. Finally, it has even been shown that individual dopaminergic neurons in the mesolimbic circuitry can respond differentially to distinct DOR agonists.[18] New analytical tools that are capable of directly monitoring rapid opioid peptide fluctuations *in situ* are needed to elucidate the contribution of individual opioid peptides to brain function.

Estimates of neuropeptide concentration are generally accomplished by coupling a sampling technique, such as microdialysis, to an *ex situ* analytical measurement of the collected fraction.[19−27] This approach is widely used for monitoring small molecule neurotransmitters, but is difficult to apply to neuropeptides. These low abundance molecules are

Special Issue: Monitoring Molecules in Neuroscience 2018

Received: July 14, 2018
Accepted: December 20, 2018
Published: December 20, 2018

DOI: 10.1021/acschemneuro.8b00351
ACS Chem. Neurosci. 2019, 10, 2022−2032

presumably released from diffuse fibers, and the probe volume is large when compared to the volume of the nerve terminal, resulting in substantial dilution as steady-state concentrations are reached. Further, microdialysis recovery efficiencies are low, particularly for "sticky" neuropeptides that readily adhere to polymeric materials (typically <5% recovery).[28] These issues are significant because the sensitivity of the detection method and the absolute recovery of the probe ultimately limit the temporal resolution.[29] Recent studies have coupled microdialysis to liquid chromatography−mass spectrometry (LC-MS)[30] to detect M-ENK in dialysate from the dorsal striatum,[21] globus pallidus,[31] and hippocampus[32] of rodents. However, this approach necessitates sampling periods of at least tens of minutes. This exacerbates the analytical challenge, as peptides are known to rapidly undergo cleavage and oxidation during sample collection.[33,34]

Background-subtracted, fast-scan cyclic voltammetry (FSCV) is commonly used to monitor DA fluctuations in the striatum during specific behavioral tasks related to reward seeking and consumption.[35−39] We previously developed a modified-sawhorse waveform (MSW) for FSCV that incorporates three different scan rates in each sweep to address several challenges associated with the electrochemical detection of tyrosine-containing peptides, such as M-ENK.[40] Herein, we systematically investigated the waveform parameters for the electrochemical detection of M-ENK in the presence of catecholamine (CA). Incorporation of the optimized parameters increased sensitivity to M-ENK by more than 3-fold and enabled simultaneous monitoring of M-ENK and CA at single, micrometer-scale recording sites in the rat dorsal striatum. The differential nature of this approach enables measurement of chemical fluctuations without interference from relatively stable or slowly changing electrochemical species that do not contribute to transient surges in chemical neurotransmitter. Thus, it provides the ability to reveal critical mechanistic details about rapid neuropeptide signaling and promises to considerably advance understanding of peptidergic mechanisms implicated in normal physiological function and in maladaptive behaviors such as drug addiction.

RESULTS AND DISCUSSION

An Introduction to the Modified Sawhorse Waveform. The classic triangular waveform that is most frequently used in FSCV cannot be used to monitor opioid peptide fluctuations because of a plethora of issues previously described by our group.[40] We overcame these limitations by designing a modified-sawhorse waveform (MSW), herein referred to as MSW 1.0 (Figure 1a). In the first segment of the forward scan, the potential is swept at 100 V s^{-1} from an accumulation potential of −0.2 V to a transition potential of +0.6 V. The scan rate is increased to 400 V s^{-1} in the second segment of the forward sweep, which terminates at +1.2 V. The potential is held for 3 ms of measurements at 1.2 V before returning to −0.2 at 100 V s^{-1}.This waveform generates separate peaks for tyrosine and methionine moieties (Figure 1b). Many peptides in the brain contain these residues; however, most of these are present at relatively constant concentrations over the time course of the measurement (tens of seconds). As such, they are subtracted with the background signal. Only a peptide that contains both tyrosine and methionine and that surges in concentration over the seconds time scale is putatively identified as M-ENK with this approach.

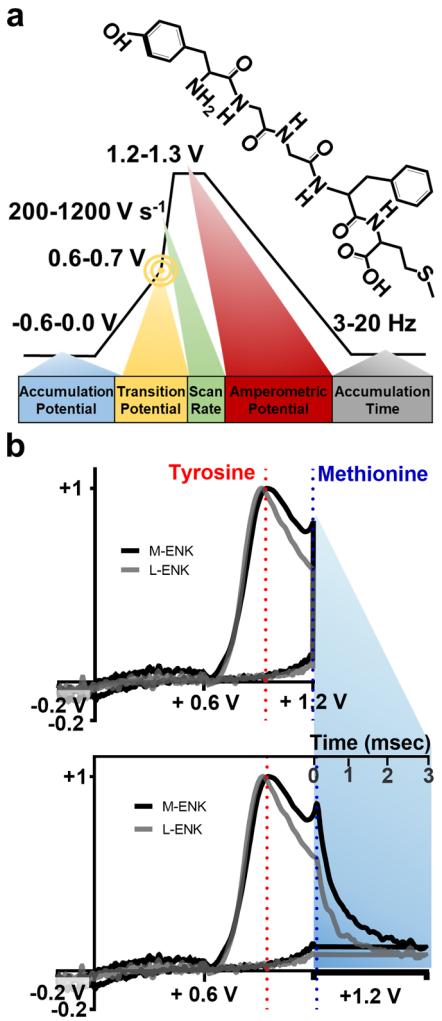

Figure 1. Introduction to the MSW. (a) A schematic of the MSW with the parameters of interest labeled. M-ENK, the target analyte, was used for waveform characterization. (b) Representative CVs (top) and mCVs (bottom) for M-ENK and L-ENK (normalized). Current collected during the amperometric period is plotted with respect to time (shaded region). M-ENK and L-ENK differ only at the C-terminus, with either a methionine or a leucine group, respectively. Both pentapeptides share the same first peak, but the presence of the second peak allows M-ENK to be visually distinguished.

In order to optimize and explore the full potential of the MSW for detection of M-ENK, the customizable waveform parameters were systematically evaluated. Application frequency, accumulation potential, scan rate, amperometric hold potential, and the transition potential that separates the first segment of the forward sweep from the second were varied to evaluate impact on electrochemical performance (Figure 1a). Individual CVs typically display potential and current on the abscissa and ordinate, respectively. As a result, current collected during the amperometric hold portion of the MSW collapses into a vertical line (Figure 1b, top). In this work, data collected during the amperometric hold were plotted with respect to hold time, using a scaling factor. The modified cyclic voltammograms (mCVs; Figure 1b, bottom) retain the conventional CV shape while also enabling visualization of currents generated during the amperometric hold period (shaded region). Chemical selectivity for M-ENK relies on the presence of distinct peaks generated in the oxidation of the

DOI: 10.1021/acschemneuro.8b00351
ACS Chem. Neurosci. 2019, 10, 2022−2032

tyrosine and methionine amino acid residues, which appear at ~0.95 V and in the amperometric hold, respectively. Plotting the data in the mCV format facilitates visualization of both peaks, even enabling M-ENK to be distinguished from the closely related pentapeptide, leu-enkephalin (L-ENK), which differs by a single amino acid (Figure 1b, bottom). Thus, the mCV convention is used throughout this work.

Waveform Application Frequency. Adsorption plays a large role in the detection of many electroactive neurochemicals. For example, DA is positively charged at physiological pH, and it has been shown to concentrate at electrode surfaces during the period between voltammetric scans, when an electrode is negatively charged.[41] Peptides contain many ionizable groups and other functionalities that influence electrochemical detection. To investigate this, the electrochemical response to 1 μM M-ENK was recorded using waveform application frequencies of 3, 5, 10, and 20 Hz, which correspond to intersweep accumulation times of 307, 174, 94, and 24 ms, respectively (Figure 2a, top). All other waveform

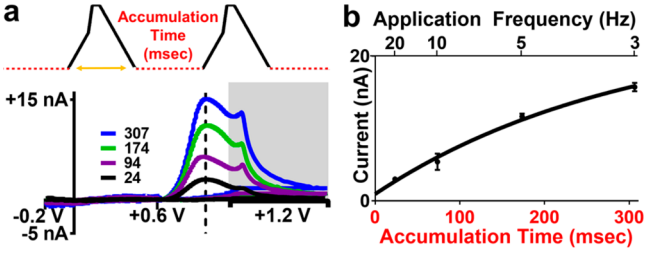

Figure 2. Waveform application frequency impacts sensitivity to M-ENK. (a) (top) Accumulation time as the MSW parameter under investigation. (bottom) Representative mCVs for bolus injections of 1 μM M-ENK. (b) Accumulation time (or application frequency) and current (tyrosine peak ~0.95 V; dotted line) plotted on the abscissa and ordinate, respectively (n = 3 electrodes). Exponential line included as a guide for the eye.

parameters were held constant. As accumulation time increased, anodic current for the oxidation of M-ENK increased (Figure 2a,b). This suggests that M-ENK concentrates on the carbon-fiber microelectrode surface between scans, thereby amplifying the signal generated upon electrolysis. The 5 Hz waveform application frequency generated substantial current while maintaining subsecond temporal resolution. Thus, unless otherwise stated, 5 Hz was chosen as the waveform application frequency for subsequent experiments.

Accumulation Potential and Scan Rate. The electrolysis of adsorption-controlled species is also impacted by accumulation potential. Thus, accumulation potential was systematically varied to investigate the impact on the voltammetric signal for M-ENK. Figure 3a (top) displays the waveforms used in this experiment. Accumulation potential was varied (0.0, −0.2, −0.4, and −0.6 V); all other parameters were held constant. Figure 3a (middle) depicts representative mCVs for 1 μM M-ENK. Figure 3a (bottom) presents a plot of the average peak current recorded in response to 1 μM M-ENK as a function of the accumulation potential (slope = −14.0 ± 0.9 nA V^{-1}, R^2 = 0.93). Peak current clearly increased as the accumulation potential decreased (became more negative), consistent with adsorption-controlled electrolysis of M-ENK.

According to the Randles−Sevcik equation, current scales with scan rate.[42] Thus, the scan rate in the potential window

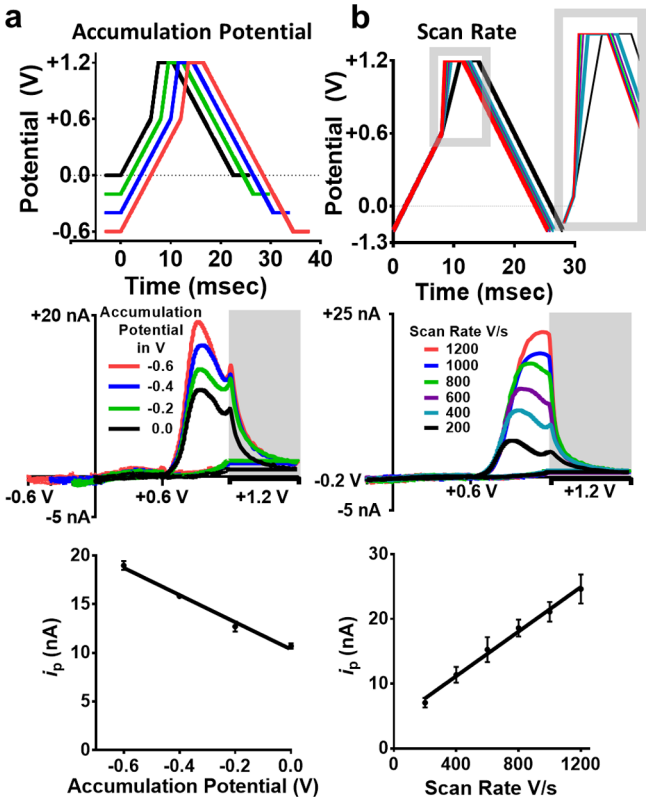

Figure 3. Characterization of the voltammetric signal for M-ENK when varying accumulation potential (a) and scan rate (b). (top) Electrochemical waveforms investigated. The inset is an enlarged view of the region of interest. (middle) Representative mCVs collected in response to 1 μM M-ENK. (bottom) Peak anodic current generated in M-ENK oxidation (~0.95 V) increased as the accumulation potential decreased and as the scan rate in the second segment of the forward scan increased (n = 5 electrodes per parameter).

for tyrosine oxidation was systematically varied. Tyrosine oxidation occurs at approximately +1 V in the second segment of the forward sweep. Figure 3b (top) highlights how changing the scan rate in this window alters the time it takes to reach the amperometric hold potential, as well as the total duration of the waveform. Representative mCVs for 1 μM M-ENK collected using scan rates from 200 to 1200 V s^{-1} in this segment of the waveform are shown in Figure 3b (middle). Figure 3b (bottom) depicts the relationship between scan rate and the peak current generated by oxidation of 1 μM M-ENK (slope = 0.0172 ± 0.0007 nA V^{-1}, R^2 = 0.99). It is important to note that increasing the scan rate shifts the peak attributed to tyrosine oxidation (at approximately +1 V), toward the amperometric hold. In fact, exceeding 800 V s^{-1} results in a complete loss of resolution, as the peaks that serve to identify the electroactive amino acids, tyrosine and methionine, completely overlap. Therefore, scan rates above 400 V s^{-1} should not be used to monitor M-ENK when using MSW 1.0.

Amperometric Potential and Transition Potential. In an attempt to recover the characteristic two-peak signature of M-ENK that was lost with incorporation of higher scan rates (Figure 3b, middle), an amperometric potential of +1.3 V was investigated. In this experiment and in all subsequent analyses, unless otherwise stated, an accumulation potential of −0.4 V, a transition potential of +0.7 V, and a scan rate of 600 V s^{-1} in the second segment of the forward scan were employed. Figure 4a (top) shows the waveforms, which incorporate an

DOI: 10.1021/acschemneuro.8b00351
ACS Chem. Neurosci. 2019, 10, 2022−2032

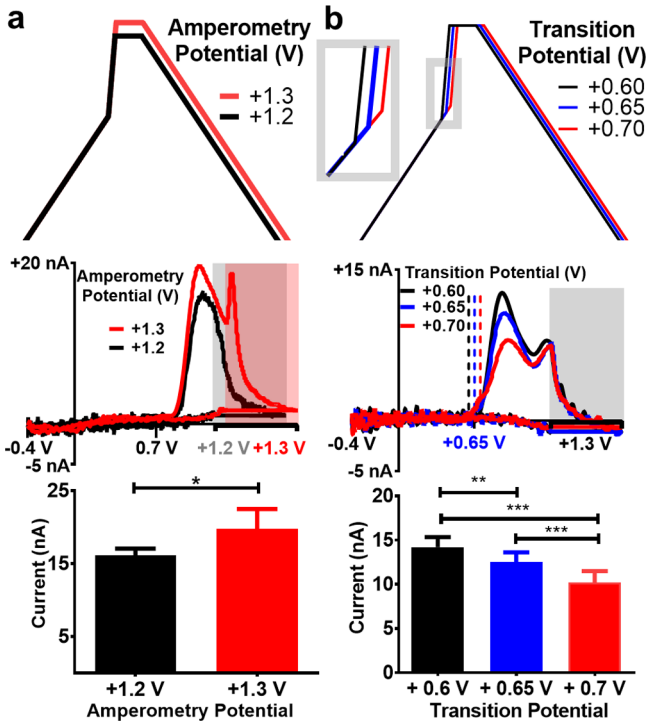

Figure 4. Potentials selected at both nodes of the second segment of the forward scan influence the voltammetric response of M-ENK. (top) Schematic of the applied waveforms used to investigate amperometric potentials of +1.2 and +1.3 V (a) and transition potentials of +0.6, +0.65, and +0.7 V (b). (middle) Representative mCVs collected for 1 μM M-ENK. (Bottom) Increasing the amperometric potential from +1.2 to +1.3 V increased the peak signal. Increasing the transition potential significantly decreased signal amplitude. *p < 0.05, **p < 0.01, ***p < 0.001; n = 5 electrodes.

amperometric potential of either +1.2 or +1.3 V. Figure 4a (middle) depicts representative mCVs for 1 μM M-ENK collected using both waveforms. The data clearly show that extending the forward sweep to +1.3 V recovers peak resolution when using higher scan rates. Furthermore, Figure 4a (bottom) demonstrates that this also improves sensitivity to M-ENK ($t(4)$ = 3.803, p < 0.05; n = 5 electrodes). Based on these results, all subsequent analyses utilized an amperometric potential of +1.3 V.

There is significant evidence that neuropeptide and small molecule neurotransmitters are copackaged within vesicles and that release can occur simultaneously.[43,44] Furthermore, estimates of CA concentrations in the extracellular space, for instance, in striatum, are much higher than estimates of opioid peptide concentrations.[21,45] Thus, CA molecules could easily interfere with the detection of low abundance peptides. The CA neurotransmitters oxidize in the +0.5 to +0.7 V range. Ideally, CA oxidation would be completed prior to reaching the second segment of the forward scan to facilitate accurate quantification of both analytes. Transition potentials of +0.6, +0.65, or +0.7 V (Figure 4b, top) were investigated with other parameters held constant. Figure 4b (middle) shows representative mCVs for M-ENK collected using the different waveforms. Increasing the transition potential resulted in a decrease in the current generated for M-ENK oxidation, as shown in Figure 4b (bottom) ($F(2, 8)$ = 95.44, p < 0.0001). However, this drawback was offset by a significant benefit.

Figure 5 displays representative mCVs for 1 μM M-ENK, 500 nM DA (physiologically relevant for work in rodent

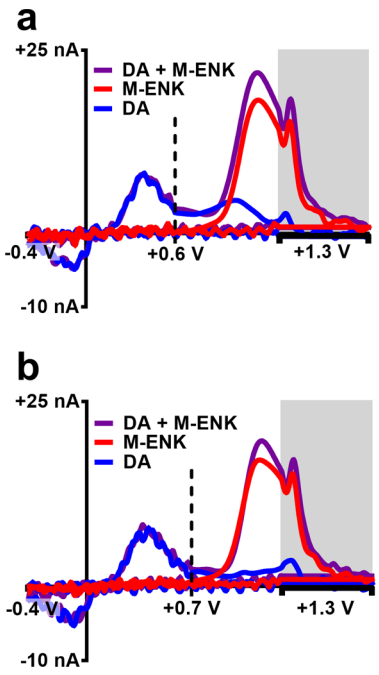

Figure 5. Transition potential that distinguishes the first segment of the forward scan from the second can be tailored to maximize sensitivity or selectivity. Representative mCVs collected with transition potentials of +0.6 V (a) or +0.7 V (b) for detection of 1 μM M-ENK, 500 nM DA, and a mixture of both species containing the same concentrations.

striatum), and a mixture of the two analytes (at the same concentrations) collected with transition potentials of +0.6 and +0.7 V. The total charge contribution to the signal collected in each segment of the forward scan was examined (excluding the amperometric hold period). The results indicate that in the mixed signal, DA contributes 28.5% ± 0.9% and 18.5% ± 0.7% of the total charge collected in the second segment of the forward scan with transition potentials of +0.6 and +0.7 V, respectively (n = 2 electrodes). Thus, increasing the voltage window of the initial segment (from +0.6 V to +0.7 V) allows for more complete electrolysis of DA. It should be noted that this issue is particularly important in adrenal tissue, where electrically stimulated CA release can substantially exceed 5 μM. Therefore, +0.7 V was selected as the transition potential for the subsequent studies. However, a trade-off clearly exists between sensitivity and selectivity, and determination of the most appropriate transition potential is dependent on the presence or absence of interfering chemical signals.

MSW 1.0 vs MSW 2.0: A Direct Comparison. Due to the coexistence of CAs and M-ENK in tissues targeted in this study (adrenal medulla and striatum),[31,46−49] subsequent recordings employed a +0.7 V transition potential. Given all of the above characterizations, a waveform referred to as MSW 2.0 was employed for tissue measurements using a 5 Hz application frequency. The potential was swept from −0.4 V to +0.7 V at 100 V s^{-1} before a faster sweep to +1.3 V at 600 V s^{-1}.The potential was then held at +1.3 V for 3 ms before returning to −0.4 V at 100 V s^{-1} (Figure 6a). MSW 2.0 improves upon the previous waveform (MSW 1.0). It results in defined and distinct tyrosine and methionine peaks vital for

DOI: 10.1021/acschemneuro.8b00351
ACS Chem. Neurosci. 2019, 10, 2022−2032

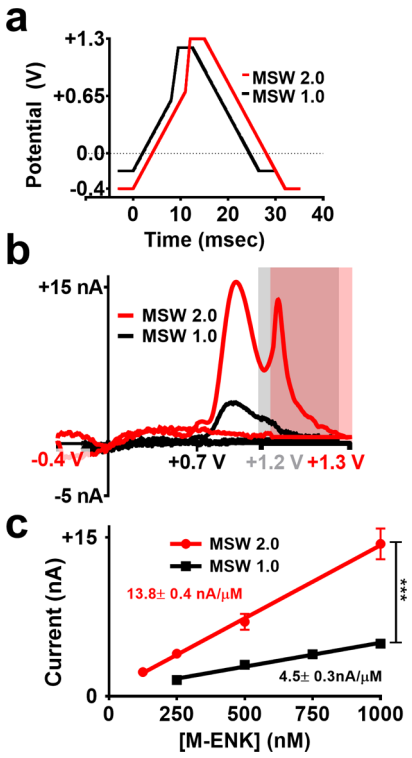

Figure 6. Improved detection of M-ENK with MSW 2.0. (a) A graphic comparison of the two waveforms. (b) Representative mCVs collected for 1 μM M-ENK using MSW 1.0[40] and MSW 2.0. (c) A direct comparison of calibration plots for M-ENK using these waveforms. ***$p < 0.001$; $n = 5$ electrodes.

chemical selectivity, as well as a greater than 3-fold increase in sensitivity (Figure 6b,c, one-way ANCOVA, $F(1, 4) = 304.9$, $p < 0.0001$; $n = 5$ electrodes).

Simultaneous Measurements of CA and M-ENK Fluctuations in Living Adrenal Tissue. Endogenous peptides are critically involved in numerous physiological functions that promote survival, including the response to stress.[6,50] For example, the electrically excitable chromaffin cells that make up the adrenal medulla secrete several neuropepides (including M-ENK) and relatively high concentrations of CAs (dopamine, norepinephrine, and epinephrine) during fight-or-flight behavior.[6,51,52] For measurements in the adrenal medulla, rats were pretreated with α-methyl-DL-tyrosine methyl ester hydrochloride (α-MPT) and reserpine to inhibit the synthesis and vesicular packaging of CAs, respectively.[53,54] This pretreatment effectively reduced CA content, in order to facilitate detection of M-ENK. Without it, the CA signal dominated the color plot, exceeding concentrations of ~5 μM (data not shown). Figure 7a displays representative color plots (top) and mCVs (bottom) for standards of 750 nM NE, 750 nM DA, and 500 nM M-ENK collected *in vitro* using MSW 2.0. Figure 7b (top) displays a representative color plot of electrically evoked CA release and a second analyte, putatively identified as M-ENK, collected in an adrenal slice (data collected at 10 Hz). A voltammogram directly following the stimulation was extracted and compared with a voltammogram for a M-ENK standard (Figure 7b, bottom). The voltammetric signature for CA is clearly evident, and there is good agreement between the normalized mCVs in the potential region where M-ENK is detected (0.7−1.3 V, $R^2 = 0.83$), providing electrochemical evidence for the identification of M-ENK. These data suggest that CA and M-ENK are released on a similar time scale upon electrical stimulation of adrenal tissue and establish the potential for MSW 2.0 in

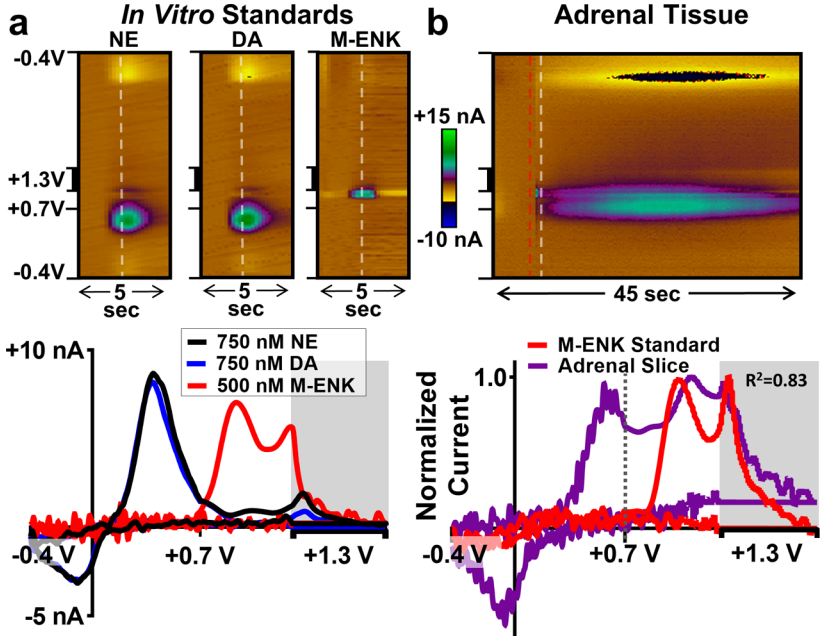

Figure 7. Simultaneous monitoring of M-ENK and CA dynamics in an adrenal slice preparation with MSW 2.0. (a) Representative data for standards of 750 nM DA and 500 nM M-ENK, and (b) M-ENK and CA released following electrical stimulation (administered at the time indicated by the red dashed line). (top) Color plots of raw voltammetric data. (bottom) mCVs extracted from the color plots at the time indicated by the white dashed line. There is good agreement between the normalized mCVs in the potential range where M-ENK is evident (to the right of the dashed line, 0.7−1.3 V, $R^2 = 0.83$).

DOI: 10.1021/acschemneuro.8b00351
ACS Chem. Neurosci. 2019, 10, 2022−2032

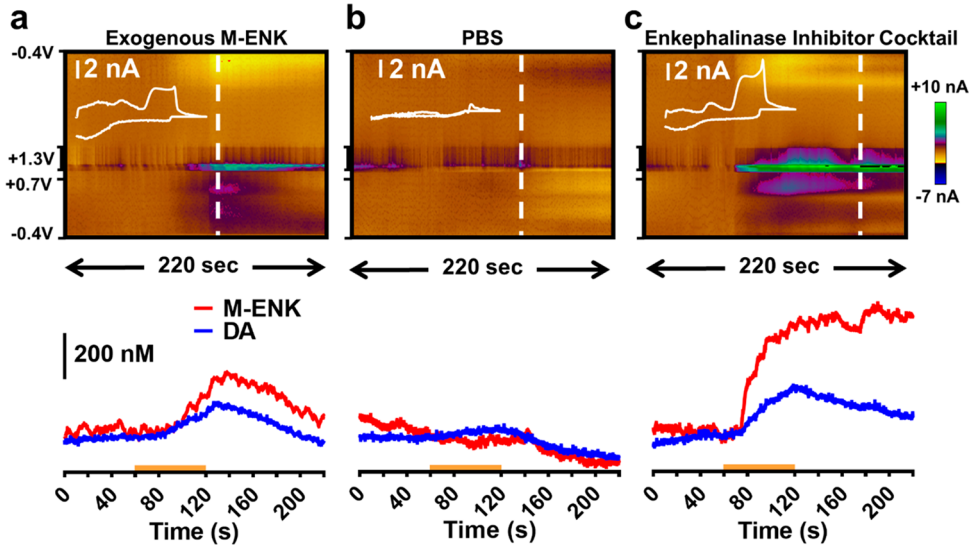

Figure 8. M-ENK recorded in the dorsal striatum of an anesthetized rat. (top) Representative color plots collected during microinfusion of M-ENK (a), PBS (b), or a cocktail of enkephalinase inhibitors (c). Infusion is marked with the orange bar on the concentration vs time plots (bottom). Inset mCVs were extracted at the time point indicated by the corresponding white dashed lines. Microinfusion of PBS did not result in any observable neurochemical changes, but local infusion of the protease inhibitor cocktail resulted in voltammograms that correlated with those collected after infusion of exogenous M-ENK (R = 0.88).

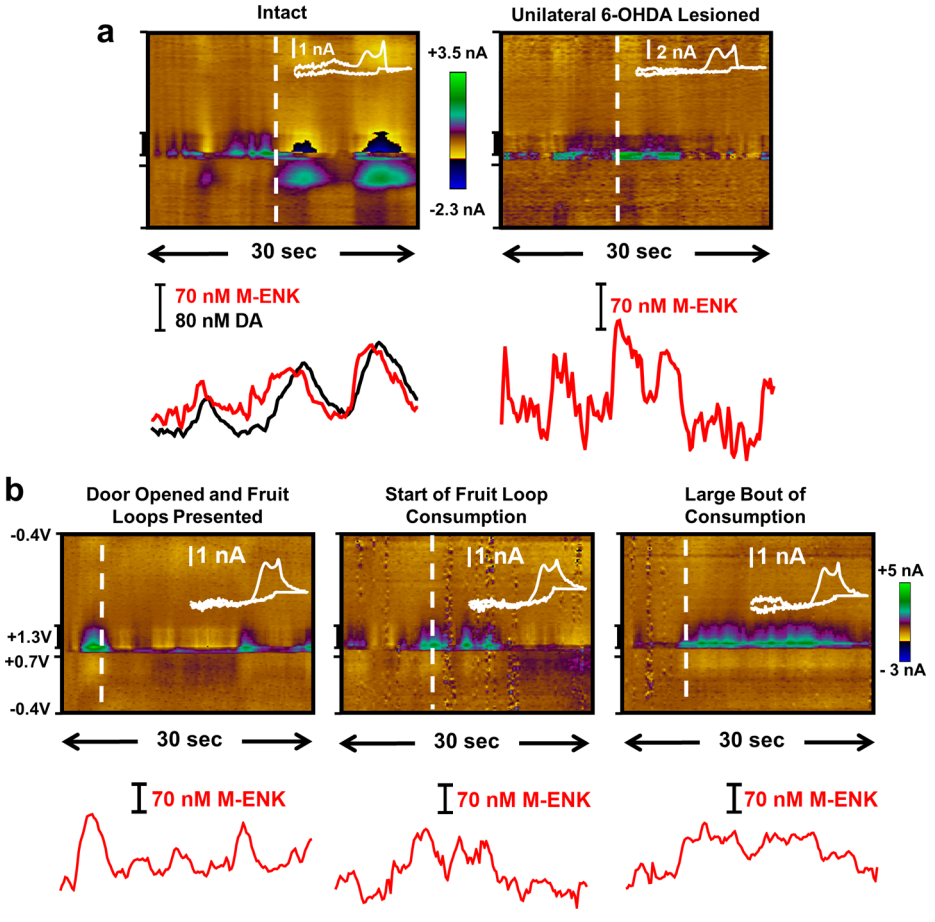

Figure 9. Neurochemical fluctuations recorded in the dorsomedial striatum of awake, freely behaving rats. Representative color plots are shown, with concentration vs time traces below. Inset mCVs were extracted at the time point indicated by the white dashed lines. (a) Voltammograms that correlate with those collected after infusion of exogenous M-ENK into striatal tissue were evident in the intact striatum (left, R = 0.85), but no CA signal was evident in the 6-OHDA lesioned animal (right). These voltammograms correlate with the M-ENK standard (R = 0.84). (b) A voltammetric signal that correlates with M-ENK fluctuations was recorded in response to the presentation (left) and consumption (middle and right) of unexpected food reward (R = 0.80−0.88).

DOI: 10.1021/acschemneuro.8b00351
ACS Chem. Neurosci. 2019, 10, 2022−2032

addressing a broad range of fundamental questions regarding endogenous opioid dynamics in live tissue.

Simultaneous Electrochemical Measurements of CA and M-ENK in the Dorsal Striatum. Enkephalins modulate motor output regions in the brain[31,55−57] and nuclei involved in food intake,[21,58] and they are involved in the integration of limbic information in the dorsal striatum.[59] Approximately 90−95% of the cellular makeup of this region consists of medium spiny neurons, approximately half of which are known to express the DA D2 receptor and various opioid receptors and to contain enkephalin.[60,61] An infusion of 1 μM M-ENK was delivered to the local vicinity of the electrode in the striatum (within ∼300−500 μm) to demonstrate the applicability of MSW 2.0 for voltammetric measurements of neuropeptide in brain tissue. Figure 8a demonstrates that MSW 2.0 can clearly detect the infused M-ENK. Interestingly, this signal was followed by an increase in extracellular CA, and the extracted mCV (inset) exhibits the defining characteristics of both CA and the M-ENK standard. Next, PBS was locally microinfused, with no observable neurochemical effects (Figure 8b). Finally, a cocktail of peptidase inhibitors was microinfused into the vicinity of the recording site (Figure 8c). This solution contained 20 μM bestatin added to a commercially available cocktail of 2 mM 4-(2-aminoethyl)-benzenesulfonyl fluoride hydrochloride, 0.3 μM aprotinin, 116 μM bestatin, 14 μM E-64, 1 μM leupeptin, and 1 mM ethylenediaminetetraacetic acid. This manipulation should locally increase the concentration and extracellular lifetime of a variety of neuropeptides. The data show a voltammetric signal consistent with that recorded for infusion of exogenous M-ENK, as demonstrated by the Pearson's correlation coefficient quantifying the covariance of the extracted mCVs (inset, R = 0.88).

When assessing a new strategy to detect endogenous molecules in the brain, an important step is to validate the approach by selectively modulating the signal using known pharmacology. However, to date, drugs to unambiguously and selectively manipulate the concentration of endogenous opioid peptides in the extracellular space do not exist. However, 6-OHDA lesioned animals exhibit increased pre-proENK mRNA expression.[62] Furthermore, because the manipulation destroys the majority of the DA neurons in the substantia nigra that project to the dorsal striatum, there is also less interference from endogenous CA. Thus, putative M-ENK signals were monitored in the dorsal striatum of an intact and a 6-OHDA lesioned rat (both awake and freely moving).

Figure 9a (left) presents a representative color plot collected in the intact animal at rest. The voltammograms (inset) are indicative of spontaneous, dynamic DA fluctuations, and there are also signals that correlate well with the voltammogram for exogenous M-ENK infused into the striatum (Figure 8a, R = 0.85). By contrast, the representative color plot collected in the 6-OHDA lesioned animal (Figure 9a, right) contains spontaneous signals consistent with voltammograms for a M-ENK standard (Figure 7, R = 0.84), with no evidence of a phasic DA signal.

Previous work has demonstrated a role for surges in ENK in the rat anterior dorsomedial striatum in the modulation of food-motivated behavior (albeit on the tens-of-minutes time scale).[21] Thus, voltammetric data were collected in anterior dorsomedial striatum of a male rat in response to unexpected palatable food reward (fruit loops, Figure 9b). Little electrochemical signal was recorded under baseline conditions, until the subject was presented with food reward. The subsequent bouts of food interaction and consumption were monitored by a trained observer while electrochemistry was recorded. The voltammograms correlate with those for the M-ENK standard (Figure 7, R = 0.80−0.88), consistent with a role for ENK surges in motivation to consume reward. Taken together, the data in Figure 9 suggest that endogenous M-ENK can be monitored in the striatum of awake animals; however, further investigation is needed to unambiguously identify M-ENK and to clarify the role that opioid peptides play in motivated behaviors.

CONCLUSIONS

Direct, real-time measurements of opioid neuropeptides in live tissue and behaving animals will provide an improved understanding of their actions in both the peripheral and central nervous systems. This work takes a significant step toward that goal. The results demonstrate that the MSW allows for direct detection of tyrosine-containing peptides, such as M-ENK, in live tissue. Through a systematic characterization of the waveform parameters, we have enhanced selectivity and sensitivity for M-ENK and demonstrated the simultaneous release of M-ENK and CA in both adrenal and striatal tissue. Importantly, this approach is not limited to endogenous opioids, and we have demonstrated how voltammetric waveforms can be customized to enhance detection of specific target analytes, broadly speaking. Overall, this work lays a foundation that can ultimately enable researchers to make direct, real-time measurements of tyrosine-containing endogenous peptides. It has the potential to enable investigation of questions concerning the specific conditions required for peptide release, peptidergic lifetime in the extracellular space, and how peptidergic flux is paired with specific behaviors. Further, the approach promises to provide valuable and unprecedented information to inform the development of therapeutic treatments of a myriad of physiological dysfunctions.

METHODS

Chemicals. All chemicals were obtained with ≥95% purity (HPLC assay) and were purchased from Sigma-Aldrich (St. Louis, MO) unless otherwise stated. The M-ENK acetate salt hydrate was obtained from LKT Laboratories (St. Paul, MN). Phosphate buffered saline (PBS; 10 mM Na_2HPO_4, 138 mM NaCl, and 2.7 mM KCl) was utilized for all *in vitro* experiments. Adrenal slice experiments were completed in bicarbonate buffered saline (BBS; 125 mM NaCl, 26 mM $NaHCO_3$, 2.5 mM KCl, 2.0 mM $CaCl_2$, 1.0 mM $MgCl_2$, 1.3 mM NaH_2PO_4, 10 mM HEPES, and 10 mM glucose) saturated with 95% O_2 and 5% CO_2. All buffers were made using ultrapure >18.2 MΩ water (Millipore, Billerica, MA) and were adjusted to pH 7.4 with 1 M NaOH and 1 M HCl.

Microelectrode Fabrication. *In vitro* and *ex vivo* electrochemical experiments were carried out with glass-insulated T-650 carbon-fiber microelectrodes (Cytec Industries, Woodland Park, NJ), fabricated as previously described.[63] Briefly, a 7-μm diameter carbon fiber was aspirated into a glass capillary, and the glass was sealed around the carbon using a micropipette puller (Narishige, Tokyo, Japan). The fiber extending past the seal was cut to 100 μm. An electrical connection with the carbon fiber was established using a high ionic strength solution (4 M potassium acetate, 150 mM KCl) to backfill the capillary. A lead wire (Squires Electronics, Cornelius) was inserted to connect the electrode to custom instrumentation.

For experiments in animals, silica-insulated carbon-fiber microelectrodes were fabricated as described previously.[64] Briefly, fused-silica tubing (90 μm outer diameter, 20 μm inner diameter) with a

DOI: 10.1021/acschemneuro.8b00351
ACS Chem. Neurosci. 2019, 10, 2022−2032

polyimide coating (Polymicro Technologies, Phoenic Arizona) was cut to 1−1.5 cm in length and placed in a bath of 70% isopropyl alcohol. A T-650 polyacrylonitrile carbon fiber was inserted through the tubing and allowed to dry. An epoxy seal (McMaster Carr, Atlanta, GA) was created at one end, and an electrical connection was completed with conductive silver epoxy (MG Chemical, Thief River Falls, MN) and a gold pin (Newark Element 14, Palatine, IL). A second layer of insulation was established around the connection using liquid insulting tape (GC Electronics, Rockford, IL). Exposed carbon fibers were cut to 100−150 μm.

For the experiments in the anesthetized animal, an "injectrode" device was fabricated, as described previously.[65] The fused silica insulation was initially cut to 3 cm (164.7 μm OD and 98.6 μm ID), and all other aspects of silica-insulated microelectrode fabrication remained unchanged. The microelectrode was placed side by side with a guide cannula (26 GA, 11 mm from pedestal; Plastics One, Roanoke, VA), and epoxy was used to secure them together as one device. Injection needles (33 GA, extending 1 mm beyond the guide; Plastics One) were positioned in the guide cannula for at least 1 min prior to infusions and remained in place for at least 1 min after infusions.

Reference electrodes were fabricated using a chloridized 0.25 mm diameter silver wire. A connection was made using a gold pin insulated with heat shrink. The silver wire and gold pin were positioned through a modified guide cannula stylet cap, and epoxy was used to secure it in place.

Electrochemical Data Acquisition *in Vitro*. All *in vitro* data were collected in a custom-built flow-injection apparatus housed within a Faraday cage. A syringe pump (New Era Pump Systems, Inc., Wantagh, NY) was utilized to enable a continuous buffer flow of 1 mL min^{-1} across the working and reference electrodes. A micromanipulator (World Precision Instruments, Inc., Sarasota, FL) allowed for precise positioning of the working microelectrode into the electrochemical cell. A Ag/AgCl pellet reference electrode (World Precision Instruments, Inc., Sarasota, FL) was used to complete the two-electrode cell. A six-port HPLC valve mounted on a two-position actuator controlled by a digital pneumatic solenoid valve (Valco Instruments, Houston, TX) enabled two-second bolus injections of analyte to be presented to the electrode.

Waveforms were applied at 3−20 Hz, and data were acquired at a sampling rate of 100 kHz using a custom-built instrument for potential application and current transduction (University of North Carolina at Chapel Hill, Department of Chemistry, Electronics Facility) or a WaveNeuro FSCV Potentiostat System (Pine Research Instrumentation, Durham, NC). High Definition Cyclic Voltammetry software (HDCV; University of North Carolina at Chapel Hill) was used in conjunction with data acquisition cards (National Instruments, Austin TX) to control waveform output, as well as to acquire and process resulting signals, including background subtraction. Electrodes in all experiments were electrochemically conditioned at 25 Hz until stable and then conditioned at the respective collection frequency needed per experiment for at least 10 additional min.

Animal Subjects and Care. Drug-naive, adult male Sprague−Dawley rats (275−300 g, Charles River Laboratories, Raleigh, NC; n = 5) were allowed to acclimate to the facility for several days. One animal received a unilateral 6-hydroxydopamine (6-OHDA) lesion of the substantia nigra by the vendor prior to receipt. Animals were individually housed on a 12:12 h light/dark cycle with free access to food and water. Animal care and use was in complete accordance with the North Carolina State University institutional guidelines (IACUC) and the NIH's Guide for the Care and Use of Laboratory Animals.

***Ex Vivo* Adrenal Slice Preparation.** Reserpine and α-MPT were prepared in 50% saline/50% dimethyl sulfoxide and in saline, respectively. Resperine (5.0 mg/kg, ip) was administered daily for 2 days prior to tissue removal and again 90 min prior to tissue removal. The α-MPT (250 mg/kg, ip) was administered 30 min prior to tissue removal. On the day of the experiment, the animal (n = 1) was deeply anesthetized with urethane (1.5 g/kg ip) and rapidly decapitated. The adrenal glands were removed and embedded in 3% agarose in BBS. The agarose gel blocks were placed in ice-cold BBS, and 400-μm thick slices were cut using a vibratome (World Precision Instruments, Sarasota, FL). Slices were allowed to rest in buffer for at least 1 h prior to placement in a recording chamber (Warner Instruments, Hamden, CT) that was superfused with BBS buffer maintained at 34 °C. They were maintained there for at least 30 min before FSCV recordings.

Glass-insulated, carbon-fiber microelectrodes were placed approximately 100 μm below the surface of each slice with the aid of a microscope (Nikon Instruments, Inc., Melville, NY), and a Ag/AgCl pellet reference electrode (World Precision Instruments, Inc., Sarasota, FL) was placed in the tissue chamber to complete the electrochemical cell. A stimulating electrode comprised of two tungsten microelectrodes (FHC, Bowdoin, ME) was positioned 1 mm away from the working electrode. Electrical stimulations were carried out with a DS-4 Biphasic Stimulus Isolator (Digitimer Ltd., Welwyn Garden City, England) controlled by the HDCV software. Stimulation consisted of 165 biphasic 500 μA pulses at a frequency of 165 Hz with a pulse width of 1.5 ms. The MSW 2.0 waveform was applied at 10 Hz for this experiment.

***In Vivo* Experiments.** Animals (n = 3) were anesthetized with isoflurane (4% for induction and 1−3% for maintenance) and surgically prepared for electrode placement, as described.[63] A heating pad (Harvard Apparatus, Holliston, MA) was used to maintain body temperature at 37 °C throughout the duration of the procedure. Briefly, holes for electrodes were drilled in the skull according to coordinates from the rat brain atlas of Paxinos and Watson.[66] A guide cannula for a Ag/AgCl reference electrode was placed in the contralateral forebrain (BASi Instruments, West Lafayette, IN). The components were permanently affixed to screws in the skull with dental cement. The animals were allowed to recover for a minimum of 4 weeks prior to experiments, with daily handling. On the day of the experiment, a fresh Ag/AgCl reference electrode was inserted into the guide cannula.

For the anesthetized animal experiments, electrochemical data were collected in the dorsal striatum (+1.6 mm anteroposterior (AP); +2.0 mm mediolateral (ML) relative to bregma; −4.5 to −5.0 mm DV from skull) using the MSW 2.0 applied at 5 Hz. On the experiment day, the animal (n = 1) was anesthetized with isoflurane (as described above), and a heating pad was used to maintain body temperature at 37 °C. The subject received intrastriatal microinfusions (0.75 μL over 1 min) of PBS or a peptidase inhibitor cocktail (20 μM bestatin HCl added to a commercially available cocktail (Sigma-Aldrich) that contained 2 mM 4-(2-aminoethyl)benzenesulfonyl fluoride hydrochloride, 0.3 μM aprotinin, 116 μM bestatin, 14 μM E-64, 1 μM leupeptin, and 1 mM ethylenediaminetetraacetic acid).

Animals used in the awake, freely behaving experiments (n = 2) were surgically prepared as described above, except silica-insulated electrodes were placed in the dorsal striatum (+1.2 mm AP, +2.0 mm ML, and −4.5 DV). The animals were allowed to recover for a minimum of 4 weeks and were handled daily. The animal used in the fruit loops experiment received fruit loops daily after surgical recovery to prevent neophobia. On the day of the experiment, the animal was tethered and connected to a head-mounted voltammetric amplifier (current-to-voltage converter), commonly referred to as a headstage (University of North Carolina at Chapel Hill, Department of Chemistry, Electronics Facility). The headstage connects to the instrumentation via a swiveling commutator (SwivElectra; Crist Instument Co., Hagerstown, MD) to permit relatively unrestricted, free movement in the custom-built plexiglass chamber. Electrochemical data were collected using the MSW 2.0 applied at 5 Hz.

Statistics and Graphics. All data presented are shown as mean ± SEM, unless otherwise noted. Paired two-tailed Student's t tests, one-way repeated measures analysis of variance (ANOVA) with Bonferonni post hoc tests or analysis of covariance (ANCOVA) tests were used where appropriate. Significance was designated at $p < 0.05$. Graphical depictions and statistical analyses were carried out using GraphPad Prism 6 or 7 (GraphPad Software, Inc., La Jolla, CA) and HDCV. MATLAB R2016a was used to convert traditional CVs to mCVs for visualizing the data, and Microsoft Excel 2013 was used to calculate correlation values.

DOI: 10.1021/acschemneuro.8b00351
ACS Chem. Neurosci. 2019, 10, 2022−2032

AUTHOR INFORMATION

Corresponding Author

*Phone: 919-515-0320. E-mail: lasomber@ncsu.edu (L.A.S.).

ORCID

L. A. Sombers: 0000-0002-0978-9795

Author Contributions

L.A.S. and G.S.M. conceived of the work, all other authors others designed experiments, collected data, analyzed data, and contributed to the preparation of the manuscript.

Funding

This work was supported by the U.S. National Institutes of Health (Grant R01-DA043007), the North Carolina State University W.M. Keck Center for Behavioral Biology, and the Department of Chemistry at North Carolina State University. S.E.C. was supported by the NIH/NCSU Molecular Biotechnology Training Program (Grant 5T32GM00-8776-15); C.J.M. is supported by an NSF Graduate Research Fellowship (Grant DGE-1252376).

Notes

The authors declare no competing financial interest.

ACKNOWLEDGMENTS

We thank James Roberts, Samantha Smith, Leslie Wilson, and Nastassja Rhodes for technical assistance and helpful discussion.

ABBREVIATIONS

MOR, mu opioid receptor; DOR, delta opioid receptor; KOR, kappa opioid receptor; LC-MS, liquid chromatography−mass spectrometry; M-ENK, methionine enkephalin; FSCV, fast-scan cyclic voltammetry; DA, dopamine; MSW, modified sawhorse waveform; CA, catecholamine; CV, cyclic voltammogram; mCV, modified cyclic voltammogram; α-MPT, α-methyl-DL-tyrosine methyl ester hydrochloride; ip, intraperitoneal; PBS, phosphate buffered saline; BBS, bicarbonate buffered saline; SEM, standard error of the mean

REFERENCES

(1) Johnson, P. I., Stellar, J. R., and Paul, A. D. (1993) Regional reward differences within the ventral pallidum are revealed by microinjections of a mu opiate receptor agonist. *Neuropharmacology 32*, 1305−1314.

(2) Smith, K. S., and Berridge, K. C. (2005) The ventral pallidum and hedonic reward: neurochemical maps of sucrose "liking" and food intake. *J. Neurosci. 25*, 8637−8649.

(3) Smith, K. S., Tindell, A. J., Aldridge, J. W., and Berridge, K. C. (2009) Ventral pallidum roles in reward and motivation. *Behav. Brain Res. 196*, 155−167.

(4) Kelley, A. E., Bakshi, V. P., Haber, S. N., Steininger, T. L., Will, M. J., and Zhang, M. (2002) Opioid modulation of taste hedonics within the ventral striatum. *Physiol. Behav. 76*, 365−377.

(5) McBride, W. J., Murphy, J. M., and Ikemoto, S. (1999) Localization of brain reinforcement mechanisms: intracranial self-administration and intracranial place-conditioning studies. *Behav. Brain Res. 101*, 129−152.

(6) Akil, H., Watson, S. J., Young, E., Lewis, M. E., Khachaturian, H., and Walker, J. M. (1984) Endogenous opioids: biology and function. *Annu. Rev. Neurosci. 7*, 223−255.

(7) Mansour, A., Burke, S., Pavlic, R. J., Akil, H., and Watson, S. J. (1996) Immunohistochemical localization of the cloned kappa 1 receptor in the rat CNS and pituitary. *Neuroscience 71*, 671−690.

(8) Le Merrer, J., Becker, J. A. J., Befort, K., and Kieffer, B. L. (2009) Reward Processing by the Opioid System in the Brain. *Physiol. Rev. 89*, 1379−1412.

(9) Gerrits, M. A., Patkina, N., Zvartau, E. E., and van Ree, J. M. (1995) Opioid blockade attenuates acquisition and expression of cocaine-induced place preference conditioning in rats. *Psychopharmacology (Berl.) 119*, 92−98.

(10) Mitchell, J. M., Bergren, L. J., Chen, K. S., Rowbotham, M. C., and Fields, H. L. (2009) Naltrexone aversion and treatment efficacy are greatest in humans and rats that actively consume high levels of alcohol. *Neurobiol. Dis. 33*, 72−80.

(11) Mitchell, J. M., O'Neil, J. P., Janabi, M., Marks, S. M., Jagust, W. J., and Fields, H. L. (2012) Alcohol consumption induces endogenous opioid release in the human orbitofrontal cortex and nucleus accumbens. *Sci. Transl. Med. 4*, 116ra6.

(12) Olive, M. F., and Maidment, N. T. (1998) Repeated heroin administration increases extracellular opioid peptide-like immunoreactivity in the globus pallidus/ventral pallidum of freely moving rats. *Psychopharmacology (Berl.) 139*, 251−254.

(13) Skoubis, P. D., and Maidment, N. T. (2003) Blockade of ventral pallidal opioid receptors induces a conditioned place aversion and attenuates acquisition of cocaine place preference in the rat. *Neuroscience 119*, 241−249.

(14) Tang, X. C., McFarland, K., Cagle, S., and Kalivas, P. W. (2005) Cocaine-induced reinstatement requires endogenous stimulation of mu-opioid receptors in the ventral pallidum. *J. Neurosci. 25*, 4512−4520.

(15) Mansour, A., Hoversten, M. T., Taylor, L. P., Watson, S. J., and Akil, H. (1995) The cloned mu, delta and kappa receptors and their endogenous ligands: evidence for two opioid peptide recognition cores. *Brain Res. 700*, 89−98.

(16) Breslin, M. B., Lindberg, I., Benjannet, S., Mathis, J. P., Lazure, C., and Seidah, N. G. (1993) Differential processing of proenkephalin by prohormone convertases 1(3) and 2 and furin. *J. Biol. Chem. 268*, 27084−27093.

(17) Lewis, R. V. (1982) Enkephalin biosynthesis in the adrenal medulla. *Adv. Biochem. Psychopharmacol. 33*, 167−174.

(18) Margolis, E. B., Fujita, W., Devi, L. A., and Fields, H. L. (2017) Two delta opioid receptor subtypes are functional in single ventral tegmental area neurons, and can interact with the mu opioid receptor. *Neuropharmacology 123*, 420−432.

(19) Freed, A. L., Cooper, J. D., Davies, M. I., and Lunte, S. M. (2001) Investigation of the metabolism of substance P in rat striatum by microdialysis sampling and capillary electrophoresis with laser-induced fluorescence detection. *J. Neurosci. Methods 109*, 23−29.

(20) Zhou, Y., Mabrouk, O. S., and Kennedy, R. T. (2013) Rapid preconcentration for liquid chromatography-mass spectrometry assay of trace level neuropeptides. *J. Am. Soc. Mass Spectrom. 24*, 1700−1709.

(21) DiFeliceantonio, A. G., Mabrouk, O. S., Kennedy, R. T., and Berridge, K. C. (2012) Enkephalin surges in dorsal neostriatum as a signal to eat. *Curr. Biol. 22*, 1918−1924.

(22) Kostel, K. L., and Lunte, S. M. (1997) Evaluation of capillary electrophoresis with post-column derivatization and laser-induced fluorescence detection for the determination of substance P and its metabolites. *J. Chromatogr., Biomed. Appl. 695*, 27−38.

(23) Haskins, W. E., Wang, Z., Watson, C. J., Rostand, R. R., Witowski, S. R., Powell, D. H., and Kennedy, R. T. (2001) Capillary LC-MS2 at the attomole level for monitoring and discovering endogenous peptides in microdialysis samples collected in vivo. *Anal. Chem. 73*, 5005−5014.

(24) Desiderio, D. M., and Zhu, X. (1998) Quantitative analysis of methionine enkephalin and beta-endorphin in the pituitary by liquid secondary ion mass spectrometry and tandem mass spectrometry. *J. Chromatogr. A 794*, 85−96.

(25) Sinnaeve, B. A., Storme, M. L., and Van Bocxlaer, J. F. (2005) Capillary liquid chromatography and tandem mass spectrometry for the quantification of enkephalins in cerebrospinal fluid. *J. Sep. Sci. 28*, 1779−1784.

(26) Dawson, R., Jr., Steves, J. P., Lorden, J. F., and Oparil, S. (1985) Reverse-phase separation and electrochemical detection of neuropeptides. *Peptides 6*, 1173−1178.

DOI: 10.1021/acschemneuro.8b00351
ACS Chem. Neurosci. 2019, 10, 2022−2032

(27) Shen, H., Lada, M. W., and Kennedy, R. T. (1997) Monitoring of met-enkephalin in vivo with 5-min temporal resolution using microdialysis sampling and capillary liquid chromatography with electrochemical detection. *J. Chromatogr., Biomed. Appl. 704*, 43−52.
(28) Roy, M. C., Ikimura, K., Nishino, H., and Naito, T. (2010) A high recovery microsampling device based on a microdialysis probe for peptide sampling. *Anal. Biochem. 399*, 305−307.
(29) Li, Q., Zubieta, J. K., and Kennedy, R. T. (2009) Practical Aspects of in Vivo Detection of Neuropeptides by Microdialysis Coupled Off-Line to Capillary LC with Multistage MS. *Anal. Chem. 81*, 2242.
(30) Baseski, H. M., Watson, C. J., Cellar, N. A., Shackman, J. G., and Kennedy, R. T. (2005) Capillary liquid chromatography with MS3 for the determination of enkephalins in microdialysis samples from the striatum of anesthetized and freely-moving rats. *J. Mass Spectrom. 40*, 146−153.
(31) Mabrouk, O. S., Li, Q., Song, P., and Kennedy, R. T. (2011) Microdialysis and mass spectrometric monitoring of dopamine and enkephalins in the globus pallidus reveal reciprocal interactions that regulate movement. *J. Neurochem. 118*, 24−33.
(32) Wilson, R. E., Jaquins-Gerstl, A., and Weber, S. G. (2018) On-Column Dimethylation with Capillary Liquid Chromatography-Tandem Mass Spectrometry for Online Determination of Neuropeptides in Rat Brain Microdialysate. *Anal. Chem. 90*, 4561−4568.
(33) Berges, J., de Oliveira, P., Fourre, I., and Houee-Levin, C. (2012) The one-electron reduction potential of methionine-containing peptides depends on the sequence. *J. Phys. Chem. B 116*, 9352−9362.
(34) Devi, L., and Goldstein, A. (1986) Conversion of Leumorphin (Dynorphin B 29) to Dynorphin B and Dynorphin B 14 by Thiol Protease Activity. *J. Neurochem. 47*, 154−157.
(35) Cameron, C. M., Wightman, R. M., and Carelli, R. M. (2014) Dynamics of rapid dopamine release in the nucleus accumbens during goal-directed behaviors for cocaine versus natural rewards. *Neuropharmacology 86*, 319−328.
(36) Willuhn, I., Wanat, M. J., Clark, J. J., and Phillips, P. E. (2010) Dopamine signaling in the nucleus accumbens of animals self-administering drugs of abuse. *Curr. Top. Behav. Neurosci. 3*, 29−71.
(37) Phillips, P. E., Stuber, G. D., Heien, M. L., Wightman, R. M., and Carelli, R. M. (2003) Subsecond dopamine release promotes cocaine seeking. *Nature 422*, 614−618.
(38) Roitman, M. F., Stuber, G. D., Phillips, P. E., Wightman, R. M., and Carelli, R. M. (2004) Dopamine operates as a subsecond modulator of food seeking. *J. Neurosci. 24*, 1265−1271.
(39) Stuber, G. D., Roitman, M. F., Phillips, P. E., Carelli, R. M., and Wightman, R. M. (2005) Rapid dopamine signaling in the nucleus accumbens during contingent and noncontingent cocaine administration. *Neuropsychopharmacology 30*, 853−863.
(40) Schmidt, A. C., Dunaway, L. E., Roberts, J. G., McCarty, G. S., and Sombers, L. A. (2014) Multiple scan rate voltammetry for selective quantification of real-time enkephalin dynamics. *Anal. Chem. 86*, 7806−7812.
(41) Heien, M., Phillips, P. E. M., Stuber, G. D., Seipel, A. T., and Wightman, R. M. (2003) Overoxidation of carbon-fiber microelectrodes enhances dopamine adsorption and increases sensitivity. *Analyst 128*, 1413−1419.
(42) Bard, A. J., and Faulkner, L. R. (2001) *Electrochemical Methods: Fundamentals and Applications*, John Wiley & Sons, Hoboken, NJ.
(43) Nguyen, T. T., and Léan, A. D. (1987) Nonadrenergic modulation by clonidine of the cosecretion of catecholamines and enkephalins in adrenal chromaffin cells. *Can. J. Physiol. Pharmacol. 65*, 823−827.
(44) Kawagoe, K. T., Garris, P. A., Wiedemann, D. J., and Wightman, R. M. (1992) Regulation of transient dopamine concentration gradients in the microenvironment surrounding nerve terminals in the rat striatum. *Neuroscience 51*, 55−64.
(45) Howe, M. W., Tierney, P. L., Sandberg, S. G., Phillips, P. E. M., and Graybiel, A. M. (2013) Prolonged dopamine signalling in striatum signals proximity and value of distant rewards. *Nature 500*, 575.
(46) Klein, R. L., Wilson, S. P., Dzielak, D. J., Yang, W. H., and Viveros, O. H. (1982) Opioid peptides and noradrenaline co-exist in large dense-cored vesicles from sympathetic nerve. *Neuroscience 7*, 2255−2261.
(47) Kelle, A. E., Stinus, L., and Iversen, S. D. (1980) Interactions between d-Ala-Met-enkephalin, A10 dopaminergic-neurons, and spontaneous behavior in the rat. *Behav. Brain Res. 1*, 3−24.
(48) Kalivas, P. W., Widerlov, E., Stanley, D., Breese, G., and Prange, A. J. (1983) Enkephalin action on the mesolimbic system - a dopamine-dependent and a dopamine-independent increase in locomotor activity. *J. Pharmacol. Exp. Ther. 227*, 229−237.
(49) Johnson, S. W., and North, R. A. (1992) Opioids excite dopamine neurons by hyperpolarization of local interneurons. *J. Neurosci. 12*, 483−488.
(50) Pasternak, G. W., and Pan, Y. X. (2013) Mu opioids and their receptors: evolution of a concept. *Pharmacol. Rev. 65*, 1257−1317.
(51) Toneff, T., Funkelstein, L., Mosier, C., Abagyan, A., Ziegler, M., and Hook, V. (2013) Beta-amyloid peptides undergo regulated co-secretion with neuropeptide and catecholamine neurotransmitters. *Peptides 46*, 126−135.
(52) Verhofstad, A. A., Coupland, R. E., Parker, T. R., and Goldstein, M. (1985) Immunohistochemical and biochemical study on the development of the noradrenaline- and adrenaline-storing cells of the adrenal medulla of the rat. *Cell Tissue Res. 242*, 233−243.
(53) Martínez-Olivares, R., Villanueva, I., Racotta, R., and Piñón, M. (2006) Depletion and recovery of catecholamines in several organs of rats treated with reserpine. *Auton. Neurosci. 128*, 64−69.
(54) Kulagina, N. V., and Michael, A. C. (2003) Monitoring Hydrogen Peroxide in the Extracellular Space of the Brain with Amperometric Microsensors. *Anal. Chem. 75*, 4875−4881.
(55) Koshimizu, Y., Wu, S. X., Unzai, T., Hioki, H., Sonomura, T., Nakamura, K. C., Fujiyama, F., and Kaneko, T. (2008) Paucity of enkephalin production in neostriatal striosomal neurons: analysis with preproenkephalin-green fluorescent protein transgenic mice. *Eur. J. Neurosci. 28*, 2053−2064.
(56) Henry, B., Crossman, A. R., and Brotchie, J. M. (1999) Effect of repeated L-DOPA, bromocriptine, or lisuride administration on preproenkephalin-A and preproenkephalin-B mRNA levels in the striatum of the 6-hydroxydopamine-lesioned rat. *Exp. Neurol. 155*, 204−220.
(57) Henry, B., Duty, S., Fox, S. H., Crossman, A. R., and Brotchie, J. M. (2003) Increased striatal pre-proenkephalin B expression is associated with dyskinesia in Parkinson's disease. *Exp. Neurol. 183*, 458−468.
(58) Pratt, W. E., and Kelley, A. E. (2005) Striatal muscarinic receptor antagonism reduces 24-h food intake in association with decreased preproenkephalin gene expression. *Eur. J. Neurosci. 22*, 3229−3240.
(59) Banghart, M. R., Neufeld, S. Q., Wong, N. C., and Sabatini, B. L. (2015) Enkephalin Disinhibits Mu Opioid Receptor-Rich Striatal Patches via Delta Opioid Receptors. *Neuron 88*, 1227−1239.
(60) Kemp, J. M., and Powell, T. P. (1971) The connexions of the striatum and globus pallidus: synthesis and speculation. *Philos. Trans. R. Soc., B 262*, 441−457.
(61) Gerfen, C. R., Engber, T. M., Mahan, L. C., Susel, Z., Chase, T. N., Monsma, F. J., Jr., and Sibley, D. R. (1990) D1 and D2 dopamine receptor-regulated gene expression of striatonigral and striatopallidal neurons. *Science 250*, 1429−1432.
(62) Gerfen, C. R., McGinty, J. F., and Young, W. S., 3rd. (1991) Dopamine differentially regulates dynorphin, substance P, and enkephalin expression in striatal neurons: in situ hybridization histochemical analysis. *J. Neurosci. 11*, 1016−1031.
(63) Roberts, J. G., Lugo-Morales, L. Z., Loziuk, P. L., and Sombers, L. A. (2013) Real-Time Chemical Measurements of Dopamine Release in the Brain, in *Dopamine: Methods and Protocols* (Kabbani, N., Ed.), pp 275−294, Humana Press, Totowa, NJ.

DOI: 10.1021/acschemneuro.8b00351
ACS Chem. Neurosci. 2019, 10, 2022−2032

(64) Clark, J. J. S., Sandberg, S. G., Wanat, M. J., Gan, J. O., Horne, E. A., Hart, A. S., Akers, C. A., Parker, J. G., Willuhn, I., Martinez, V., Evans, S. B., Stella, N., and Phillips, P. E. M. (2010) Chronic microsensors for longitudinal, subsecond dopamine detection in behaving animals. *Nat. Methods 7*, 126−129.
(65) Wilson, L. R., Panda, S., Schmidt, A. C., and Sombers, L. A. (2018) Selective and Mechanically Robust Sensors for Electrochemical Measurements of Real-Time Hydrogen Peroxide Dynamics in Vivo. *Anal. Chem. 90*, 888−895.
(66) Paxinos, G., and Watson, C. (2006) *The rat brain in stereotaxic coordinates*, hard cover ed.; Elsevier.

DOI: 10.1021/acschemneuro.8b00351
ACS Chem. Neurosci. 2019, 10, 2022−2032